

VYTAUTAS BARZDAITIS *, VYTAUTAS ŽEMAITIS **, V.V. BARZDAITIS ***,
RIMANTAS DIDŽIOKAS****

STABILITY OF ROTOR WITH GAS-LUBRICATED JOURNAL BEARING

The paper presents research on dynamics, modeling and the results of experimental tests of the rotor system rotating in gas lubricated bearing with a floating bush. The dependence of rotor vibration intensity on the waviness of bearing elements was tested and simulated. It was confirmed experimentally that the amplitude of rotor vibration in gas lubricated bearing with double gas film is basically lower than the one with single gas film. The kinetic orbits of the rotor shaft vibration displacements are presented. Dynamic and mathematical models constructed enable to design bearings that distinct optimal according to the minimal vibration intensity.

1. Introduction

The intensity of the vibration of rotor systems is one of the main parameters of their suitability, especially in the high speed machines and precision systems. The intensity of the vibration of rotor systems is reduced technologically when increasing the accuracy of the manufacturing of the bearing elements working surfaces. Such a way of vibration intensity reduction is explained by the quality of bearings, which depends on the deflection of a cylindrical working surfaces' geometrical form.

Another way of vibration intensity reduction is the improvement of bearings design. In paper [1], a new type of floating bush aerostatic journal bearing for an internal grinder used in manufacturing microtested bearings

* Kaunas University of Technology, Mickevičiaus st. 37, 44244 Kaunas, Lithuania; E-mail: vytautas.barzdaitis@ktu.lt

** Kaunas University of Technology, Mickevičiaus st. 37, 44244 Kaunas, Lithuania; E-mail: vytautas.zemaitis@ktu.lt

*** Vytautas Magnus University, Vileikos 8, Kaunas, LT-3035, Lithuania; E-mail: v.barzdaitis@if.vdu.lt

**** Klaipeda University, Bijunu st. 17, 5802 Klaipeda, Lithuania; E-mail: rididz@lrs.lt

is proposed. In this paper, the stability of a rigid rotor supported by the proposed bearings is modeled theoretically and experimentally.

The usage of gas bearings is essential for technological machines. For example the bearings of turboexpander of natural gas can be lubricated by gas [2].

In the past, the rotors rotating in magnetic bearings of a turboexpander failed reaching the proper rotational velocity due to the stability problem. When the magnetic bearings were changed by the ones with a gas film, the proper velocity was reached.

The purpose of this work is the theoretical and experimental research towards reduction of the vibration intensity of the rotor with the double-rowed bearing.

2. The subject of research

The gas lubricated bearing – rotor scheme with a floating bush is shown in the Fig. 1. The double-rowed bearing is designed with the circular diaphragm type restrictors and has a bearing parameter $L/D = 1,2$, where L – the length of a shaft, D – its diameter. Gas pressure in the injection chamber is $p = 0.24$ MPa.

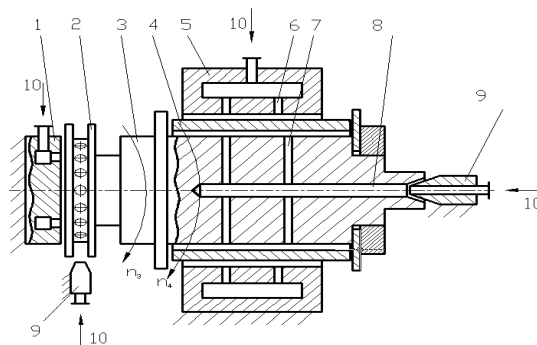


Fig. 1. The rotor scheme of a gas lubricated bearing with a floating bush: 1 – thrust bearing (fixed); 2 – gas turbine; 3 – the rotor of which dynamics is investigated; 4 – floating bush; 6, 7 and 8 – gas feeding grooves; 9 – the nipple of air supply; 10 – gas feeding to the bearing

3. Test of bearing dynamics

Experimental and theoretical methods and means were applied for the study of dynamics of the rotor system represented. The aim of experimental test was to evaluate theoretically that the radial vibration in the case of the rotor with the double film bearing is several times lower in comparison with

the single-film bearing, and to measure kinetic orbits of the rotor. The aim of theoretical modeling was to optimize the parameters of the rotor and its elements so that the vibration intensity in the case with double gas film bearing would be the least.

3.1. Technique of experimental tests

The modern testing equipment was applied for the purpose of experimental measurements, the software MMS 6000 [3] run with the machine dynamics analyser DMA 04 as presented in Fig. 2. The radial vibrations of the rotor were tested by two eddy-current contactless displacement measurement sensors 12, 13, the rotating velocity of the rotor was tested by laser type keyphasor sensor 11, and the bearing housing vibrations were tested by the seismic transducer 14. The rotating velocity of the rotor was changed in a wide range up to 4000 rpm. The vibration displacement values s_{ppx} and s_{ppy} of rotor 3 were measured in two perpendicular directions, kinetic orbit of the bearing and its maximum value of shaft displacement from time-integrated mean position “zero” s_{max} was designed according ISO 7919 recommendations. The vibration displacements $s_{1x}(t)$ and $s_{1y}(t)$ were tested by proximity sensors 1X and 1Y within the whole velocity range.

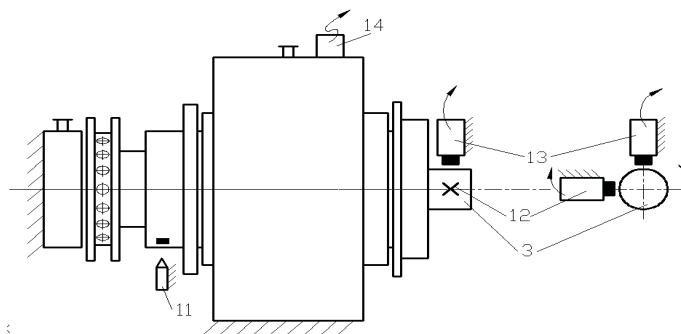


Fig. 2. The rotor scheme for the experimental tests: 3 – rotor; 11 – the laser sensor for the measurement of rotating velocity and vibration phase; 12, 13 – horizontal and vertical eddy-current sensors for the measurement of vibration displacement, 1X and 1Y; 14 – seismic transducer for the measurement of absolute vibration of the bearing housing

$$s_{\max}(t) = \sqrt{s_{1x}^2(t) + s_{1y}^2(t)} \quad (1)$$

The vibration displacement test method and the scheme running the software capacitates getting maximum vibration displacement value s_{ppmax} according Standart ISO 7919. The overall value of displacement was $s_{ppmax} = 2 \cdot s_{max}$.

3.2. Test results

The experimental tests of dynamics of the rotor system were carried out in two ways. The first test was carried out with the rotor with a single film bearing. The rotor rotated in the external gas film together with the floating bush. In the second test, the rotor with the double film bearing is used. The second gas film between the rotor and floating bush was formed. The rotating system was tested with forcing of gas turbine 2 and without it. This test provided data expressing the influence of the external load generated by the gas turbine on the vibration intensity, Fig. 1.

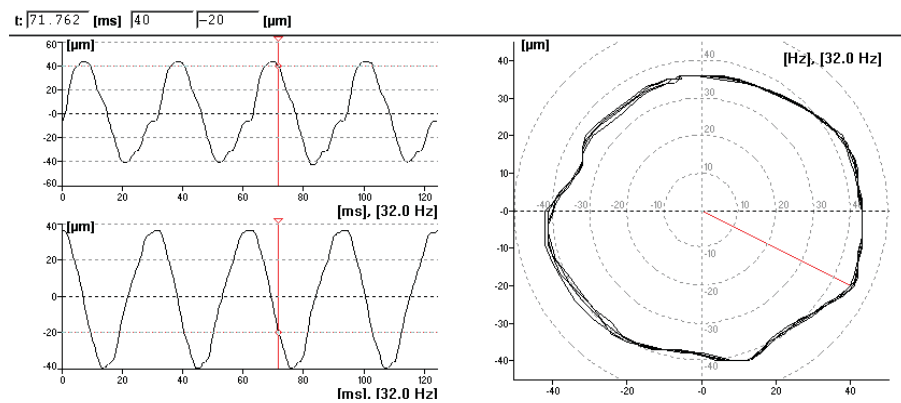


Fig. 3. The vibration displacement plots $s_{1x}(t)$ and $s_{1y}(t)$ and shaft displacements kinetic orbit with $s_{max} = 45 \mu\text{m}$ of the rotor with a single gas film

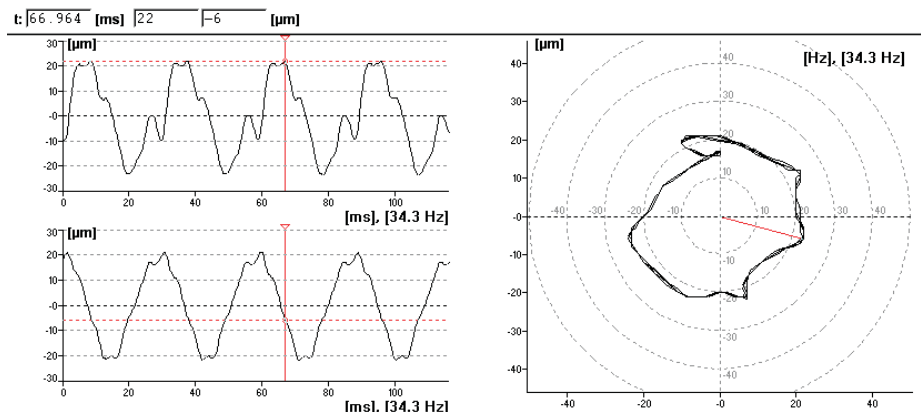


Fig. 4. The vibration displacement plots $s_{2x}(t)$ and $s_{2y}(t)$ and shaft displacements kinetic orbit with $s_{max} = 23 \mu\text{m}$ of the rotor with a double gas film

The vibration data formats presented in Fig. 3 are obtained when the vibration displacements $s_x(t)$ and $s_y(t)$ were measured in the directions X and

Y. The kinetic vibration displacement orbit s_{max} for the single film bearing, is also shown. Similar graphs in Fig. 4 pertain to the rotor running with the double film bearing.

The measured vibration characteristics confirm that in the case of double film bearing the amplitude s_{max} of the rotor system vibration displacements is twice lower in comparison with the single film bearing. In the case of a single film bearing, the bush rotating together with the shaft increases the unbalance of the rotor. The dominant harmonic vibration is generated by a unbalance and can be distinguished in the vibration displacements plots, Fig. 3.

In the case of a double film bearing running with frequency $1X=34$ Hz, vibration displacement has not only $1X$ frequency component, but there is also a noticeable additional $2X$ frequency vibration that confirms the presence of the gaps in the rotor system.

The $2X$ frequency is the sign of the misalignment of holes – gas lubricated bearing caused by ovality and conicality of the cylindrical surfaces.

4. The modeling and testing of a bearing

On the basis of experimental tests, the model was corrected and the test of the gas lubricated bearing dynamics was continued. The aim was to optimize the parameters of the rotor system with the gas lubricated bearing, which would allow us to foresee the optimal design of the minimal vibration intensity of the rotor.

4.1. Dynamic and mathematical models

Experimental tests of the rotor make it possible to correct the dynamic model of the rotor rotating in a gas lubricated bearing that is presented in the Fig. 5. The dynamic model allows us to assess: the waviness of the cylindrical working surfaces of the bearing; aerodynamic phenomena that take place between the elements of the rotor and the impact on the intensity of the rotor vibration.

The errors of the geometrical forms of the bearing cylindrical internal surfaces are much more significant than the ones of the waviness of the cylindrical external surfaces. It is due to lower stiffness of the system “machine-tool-part” and greater vibration amplitudes appearing in the process of machining holes compared to those in the processing technology of the external surface. Therefore, only the waviness of the bearing internal surfaces was taken into account in the presented model.

Taking into account the above assumption and the results of the experimental tests, we can express aerodynamic interaction force between the rotat-

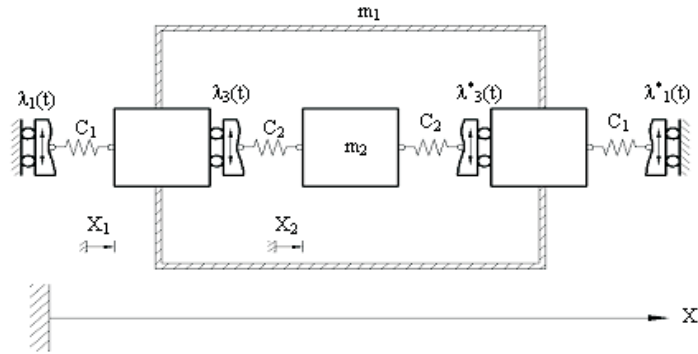


Fig. 5. The dynamic model of the rotor rotating in the gas lubricated floating bush journal bearing: m_1, m_2 – masses of the floating bush and rotor, respectively; $\lambda_1(t), \lambda_1^*(t)$ – waviness of the internal surface of the bearing housing; $\lambda_3(t), \lambda_3^*(t)$ – waviness of the internal surface of the floating bush; C_1, C_2 – stiffness coefficients of the external and internal gas films; x_1, x_2 – the floating bush and rotor displacements

ing elements of the gas lubricated journal bearing by the following equation [4]:

$$T = a \cdot h^{-n}, \quad (2)$$

where: a – coefficient, receivable $a = 1.25 \cdot 10^{-4}$; h – the gap between the working surfaces of the bearing elements; n – power index, receivable $n = 1.34$.

The mathematical model of the investigated system [4]:

$$\begin{cases} \Phi_1 - R_{C1} + R_{C2} - R_{C2}^* + R_{C1}^* - T_{C1} + T_{C2} - T_{C2}^* + T_{C1}^* = P_1, \\ \Phi_2 - R_{C2} + R_{C2}^* - T_{C2} + T_{C2}^* = P_2 \end{cases} \quad (3)$$

where: $\Phi_1 = m_1 \cdot \ddot{x}_1, \Phi_2 = m_2 \cdot \ddot{x}_2$ – inertia forces;

$$\begin{aligned} R_{C1} &= b_1 \cdot [\dot{x}_1 - \dot{\lambda}_1(t)], R_{C1}^* = b_1 \cdot [-\dot{x}_1 - \dot{\lambda}_1^*(t)], \\ R_{C2} &= b_2 \cdot [\dot{x}_2 - \dot{x}_1 - \dot{\lambda}_3^*(t)], R_{C2}^* = b_2 \cdot [\dot{x}_1 - \dot{x}_2 - \dot{\lambda}_3(t)] \end{aligned} \quad \text{– resistance forces;}$$

$T_{C1}, T_{C1}^*, T_{C2}, T_{C2}^*$ – aerodynamic interaction forces between the working surfaces of the bearing elements;

$P_1 = P_{1a} \cdot \sin(\omega_2 t + \varphi_2), P_2 = P_{2a} \cdot \sin(\omega_1 t + \varphi_1)$ – centrifugal forces induced by the unbalance of floating bush and rotor;

$\lambda_1(t), \lambda_3(t), \lambda_1^*(t), \lambda_3^*(t)$ – internal surface waviness presented in the form of Fourier series;

m_1, m_2 – the masses of the floating bush and rotor; h_{01}, h_{02} – initial gaps between the bearing housing and floating bush and between the bush and rotor; b_1, b_2 – coefficients of proportionality; ω_1, ω_2 – angular velocities of floating bush and rotor.

Mathematical model – the system of the differential equations takes the following form:

$$\begin{aligned}
 & \{\ddot{x}_1 + S_{11} \dot{x}_1 + S_{12} \dot{x}_2 + S_{13} [h_{01} + x_1 - \lambda_1(t)]^{-n} + S_{14} [h_{02} - x_1 + x_2 - \lambda_3(t)]^{-n} + \\
 & + S_{15} [h_{02} + x_1 - x_2 - \lambda_3^*(t)]^{-n} + S_{16} [h_{01} + x_1 - \lambda_1^*(t)]^{-n} = S_{17} \sin \omega_2 t + \\
 & + S_{18} \cos \omega_2 t + S_{19} \sum_1^N B_i i \sin i \omega_2 t + S_{10} \sum_1^N A_i i \cos i \omega_2 t + \\
 & + S_{111} \sum_1^N K_i i \sin i (\omega_1 - \omega_2) t + S_{112} \sum_1^N D_i i \cos i (\omega_1 - \omega_2) t; \\
 & \ddot{x}_2 + S_{21} \dot{x}_1 + S_{22} \dot{x}_2 + S_{23} [h_{02} + x_2 - x_1 - \lambda_3(t)]^{-n} + \\
 & + S_{24} [h_{02} - x_2 + x_1 - \lambda_3^*(t)]^{-n} = S_{25} \sin \omega_1 t + S_{26} \cos \omega_1 t + \\
 & + S_{27} \sum_1^N K_i i \sin i (\omega_1 - \omega_2) t + S_{28} \sum_1^N D_i i \cos i (\omega_1 - \omega_2) t.
 \end{aligned}$$

4.2. Test results

The waviness amplitudes of the inner cylindrical working surfaces of the gas lubricated bearing were measured experimentally, and the following values obtained: floating bush – $h_{a1} = 0.9 \mu\text{m}$, and the bearing housing – $h_{a2} = 1.1 \mu\text{m}$, and the wave numbers of: floating bush – $k_1 = 2$, and bearing housing – $k_2 = 3$.

The results of calculation are presented in the Fig. 6.

As it can be seen in Fig. 6, if the number of waves of the bearing housing internal surface is even, the amplitude of rotor vibration considerably declines and is independent of the amplitude of waviness; and if the number of waves is odd, the vibration amplitude increases when the amplitude of the waviness increases.

Given even number of waves of the bush internal surface and fixed amplitude of its waviness (Fig. 6b, $k_1 = 2$ and $h_{a1} = 2 \mu\text{m}$), the nature of geometrical influence of bearing housing internal surface shifts: given even number of waves of the bearing housing internal surface, the amplitude of rotor vibration is considerably lower comparing to the one in the previous figure (Fig. 6a). When the number of waves of the bearing housing is odd,

the vibration amplitude obtains lower values comparing to the ones of the odd number of the waves of the bush internal surface.

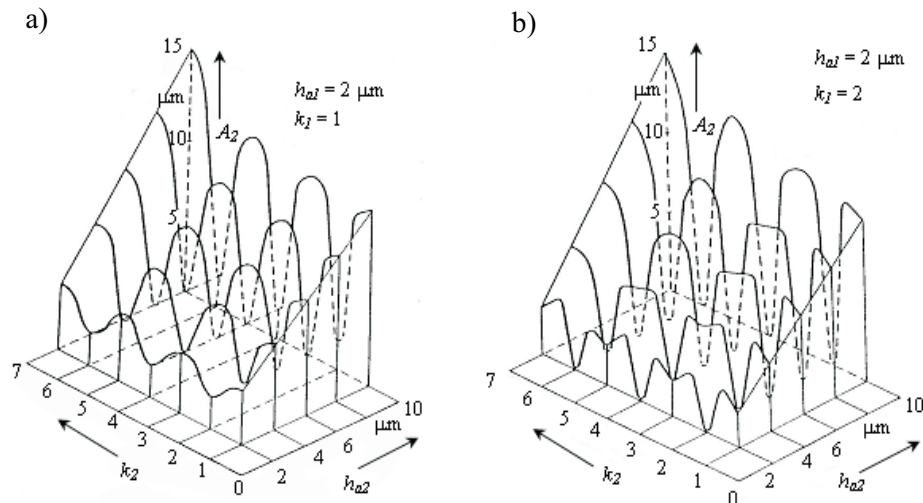


Fig. 6. Plots of the amplitudes of the rotor vibration displacements on internal surface of the bearing housing: a) $k_1 = 1$; $h_{a1} = 2 \mu\text{m}$; b) $k_1 = 2$; $h_{a1} = 2 \mu\text{m}$; h_{a1} , h_{a2} and k_1 , k_2 – waviness amplitudes and the numbers of waves of the floating bush and bearing housing internal surfaces, respectively; A_2 – the amplitudes of the rotor vibration displacements

Analysing the results of the given theoretical research, the following conclusion can be drawn: gas lubricated floating bush journal bearing, the internal bearing housing and bush surfaces of which one obtains even number of waves, exhibit the least intensity of vibration displacements.

5. Conclusions

The tested and modelled rotor with gas lubricated bearing with double film has more than twice lower vibration intensity than that with the single film bearing.

The advantage of the design of the double film bearing is confirmed by the experimental results obtained in kinetic orbits vibration data format.

Minimal vibration activity distinguishes bearing which internal surfaces of the bearing housing and bush have even number of waves.

REFERENCES

- [1] Yoshimoto S., Anno Y., Iiya T.: Floating bush aerostatic journal bearing employing slot restrictors. Proceeding of 3rd International Conference on Rotor Dynamics, 1990, pp. 99-103.

- [2] Bently D. E., Hatch Ch. T.: Stability Analysis and Initial Testing of Pressurized Gas Bearings in a 160 HP Natural gas Turboexpander.-Proc. of the Third International Symposium on Stability Control of Rotating Machinery, ISCORMA, Cleveland, Minden, 2005, pp. 309÷319.
- [3] Dynamic Machinery Analyzer DMA 04, EPRO, Elektronik & Systemtechnik GmbH Machine monitoring System (MMS), D-48599, Gronau, Germany, 2004, third edition 6110-00004, p. 50.
- [4] Žemaitis V.: Research and development of an aerostatic floating bush journal bearing. Ph.D. thesis. Kaunas, 1989. p. 116.

Stabilność wirnika z łożyskiem poprzecznym ze smarowaniem gazowym

Streszczenie

W artykule przedstawiono badanie dynamiki, modelowanie i wyniki testów eksperymentalnych zespołu wirnika obracającego się w łożysku z tuleją pływającą ze smarowaniem gazowym. Testowano i symulowano zależność intensywności wibracji od falistości powierzchni elementów łożyska. Potwierdzono eksperymentalnie, że amplituda wibracji wirnika w łożysku ze smarowaniem gazowym z podwójną warstwą gazu jest zasadniczo mniejsza od tej, jaka występuje w łożysku ze smarowaniem gazowym z pojedynczą warstwą gazu. Przedstawiono orbity kinetyczne wibracji wału wirnika. Skonstruowane modele dynamiczne i matematyczne umożliwiają projektowanie łożysk o optymalnych właściwościach wibracyjnych.